ISSN 0023-1584, Kinetics and Catalysis, 2010, Vol. 51, No. 1, pp. 10–17. © Pleiades Publishing, Ltd., 2010.
Original Russian Text © V.N. Snytnikov, T.I. Mishchenko, Vl.N. Snytnikov, O.P. Stoyanovskaya, V.N. Parmon, 2010, published in Kinetika i Kataliz, 2010, Vol. 51, No. 1, pp. 12–20.

Autocatalytic Gas-Phase Ethane Dehydrogenation in a Wall-less Reactor

V. N. Snytnikov, T. I. Mishchenko, Vl. N. Snytnikov, O. P. Stoyanovskaya, and V. N. Parmon

Boreskov Institute of Catalysis, Siberian Branch, Russian Academy of Sciences, Novosibirsk, 630090 Russia

e-mail: snyt@catalysis.ru

Received September 17, 2008

Abstract—The thermal gas-phase pyrolysis of ethane was studied under conditions of the bulk heating of the reaction mixture with IR-laser radiation. The concentrations of ethane pyrolysis products as functions of reaction time were calculated in accordance with standard kinetic schemes; they showed that a classical radical chain mechanism corresponded to only highly dilute mixtures of ethane with an inert gas. As found by calculations, the experimental data on the kinetics of consumption of the initial substance and on the kinetics of buildup of pyrolysis products in undiluted mixtures of ethane and its conversion products were adequately described by an autocatalytic (with respect to ethylene) mechanism of ethane dehydrogenation. This mechanism involved the step of ethane interaction with ethylene to form methyl and propyl radicals.

DOI: 10.1134/S0023158410010039

INTRODUCTION

The endothermic pyrolysis (dehydrogenation) of ethane via the reaction

$$C_2H_6 \longrightarrow C_2H_4 + H_2$$

to obtain ethylene belongs to the most needed chemical processes of current industry. Because of this, the pyrolysis of ethane has been studied over a wide range of conditions with the use of various pyrolysis reactor designs. In particular, this reaction has been studied at low conversions in closed reactors where thermal energy was supplied by heating the reactor walls [1–3]. Under these conditions, pyrolysis mainly occurred through homogeneous–heterogeneous steps with the participation of reactor walls. The gas-phase dehydrogenation of ethane at high temperatures, in particular, under the homogeneous conditions of shock waves in lean mixtures of ethane with inert gases has also been studied [4]. The plasma-chemical pyrolysis of ethane, in particular, in an electric arc discharge, is also a high-temperature process [5]. The inhibition and initiation of chemical transformations of ethane in the presence of other hydrocarbons have been studied [3]. Photochemical processes occurring in ethane under the action of UV radiation have been examined [6].

The gas-phase pyrolysis of ethane is a typical example of radical chain reactions [1–8]. In particular, this point of view is based on the detection of intermediate free radicals, for example, in lean ethane mixtures with inert gases at high temperatures [4]. At the same time, in the calculations of processes that occur in pyrolysis furnaces, molecular steps are usually added to the reactions taken into consideration [9] or empirical dependences of the rates of ethane consumption and product formation are used [1]. The theoretical models of ethane pyrolysis include to 100 [4] or even more than 2000 elementary steps [9].

Interest in the practically important processes of the pyrolysis of concentrated C_2–C_4 hydrocarbons and their mixtures of different compositions at high conversions in the absence of ballast inert gases has quickened in the past few years. The aim of this work was to study the gas-phase dehydrogenation of ethane in mixtures with ethylene at atmospheric pressure over the temperature range of 500–800°C under conditions such that the rate of endothermic reactions was not restricted by the finite rate of thermal energy supply to the reactor. In particular, this condition can be met with the use of a powerful laser radiation beam, which is absorbed by a gas immediately in the reaction zone volume. Thus, we managed to implement the concept of a wall-less reactor proposed as early as the 1980s [10]; in this reactor, the occurrence of near-wall processes in the course of gas-phase reactions is excluded.

EXPERIMENTAL

Radiation from a continuous-wave CO_2 laser with the wavelength $\lambda \approx 10.6$ μm was used as an energy source for endothermic processes. Lower paraffins do not absorb this radiation. However, the spectra of the unsaturated products of ethane pyrolysis—ethylene and propylene—exhibit absorption bands in the laser generation range. Thus, the experiments were based on the use of the sensitizing properties of these products at laser generation wavelengths.

Figure 1 shows the schematic diagram of the experimental setup for studying the pyrolysis of ethane. The reactor was a 6-cm^3 cylindrical quartz cell with the

inner diameter $D = 16$ mm and the length $L = 30$ mm. Radiation was supplied to the reactor volume through a window of an antireflection plane-parallel ZnSe plate (*4*). Plate *5* of GaAs with a reflection factor of ≈70% at the wavelength $\lambda = 10.6$ μm was mounted at the reactor escape. This allowed us to enhance the uniformity of radiation absorption along the cell and to measure the energy absorbed in the volume.

The body of the reactor has three locks. One of them, which was closed with a silicone stopper, was used to take samples for chromatographic analysis. The other two allowed us to replace the gas mixture in the reactor. For this purpose, the chamber was washed with a flow of a mixture of ethane and ethylene in a ratio adjusted by a UFGP gas flow controller [11]. After a pressure of 1 bar was reached in the reactor, the locks were closed and the supply of gases was stopped. The laser irradiation time of the mixture was varied from 1 to 20 s (to within ±0.1 s). When the pressure in the chamber exceeded 1 bar, an excess of gases was released into the atmosphere providing the absence of a backward flow of the atmospheric gas into the chamber. The chromatographic analysis of gas samples was performed before and after irradiation. A Hamilton gas syringe was used to take the samples. The concentrations of C_1–C_4 hydrocarbons and H_2 were determined on Kristall 2000 M and LKhM-80 MD chromatographs (Russia).

The continuous-wave CO_2 laser with the maximum radiation power $W = 130$ W was developed and made by the authors. The applied radiation power with a transverse distribution close to the TEM_{00} main mode was varied from 10 to 100 W. The active medium length was 200 cm; the radiation beam diameter at the laser outlet was $d_0 \approx 9$ mm. A spherical copper mirror and a plane-parallel plate of gallium arsenide were arranged in the resonator. As a rule, radiation was generated at one or two vibrational–rotational transitions of the CO_2-laser amplification band in the region of 930–970 cm. Note that the maximum position of the most intense absorption band of ethylene approximately corresponds to a wavenumber of 949 cm^{-1}.

Radiation power was measured with separating plates of ZnSe using an LM-2 standard instrument (Germany) with a time resolution of 2.5 s. To measure radiation energy at the reactor outlet, calorimeter *7*, which was made based on a thermoresistor sensor, with a power integration time of no shorter than 1 min was used.

Our preliminary experiments, in which the absorption of radiation with a power of 20 W in ethylene and its mixtures with methane at pressures P from 10 to 760 Torr, and an analysis of published calculation data [12] indicated that the interaction of radiation with a gas can be affected by radiation diffraction in the gas and the collision relaxation of excited molecules in a buffer gas, as well as the temperature dependence of the absorption coefficient and the photoinduced bleaching of the medium. Therefore, under conditions

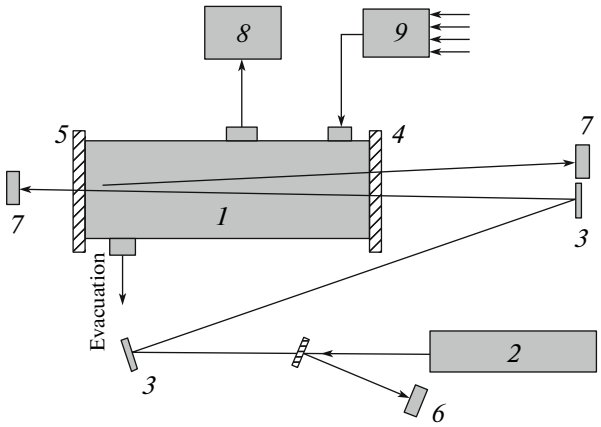

Fig. 1. Setup for studying ethane pyrolysis in a wall-less reactor: (*1*) reactor, (*2*) CO_2 laser, (*3*) optical train mirrors, (*4*) optical window of ZnSe, (*5*) semitransparent window of GaAs, (*6*) LM-2 radiation power meter, (*7*) radiation energy meter, (*8*) chromatographs, and (*9*) UFGP-4 gas flow controller.

of our reactor, absorption coefficients can differ from calculated values obtained based on the standard spectra of ethylene [13], which were measured at radiation power densities of about 1 mW/cm^2. Based on measurement data, the absorption coefficient of ethylene in the reactor used was estimated at $\alpha \approx 3.6 \times 10^{-3}$ cm^{-1} $Torr^{-1}$ (or $\alpha \approx 10^{-19}$ cm^{-2} at $T \approx 300$ K). These data are consistent with the well-known spectroscopic characteristics of ethylene.

RESULTS

In the experiments on ethane pyrolysis, we varied the power of laser radiation, the volume fraction of ethylene in the starting mixture, and the irradiation time of the reaction mixture. The starting mixture occurred at room temperature. The main pyrolysis products were C_2H_4, CH_4, and H_2. The fraction of the other detected products (C_2H_2 and C_3H_6) was <1 vol %.

Figure 2 shows the dependence of the conversion of ethylene on energy absorbed in the reactor at radiation input powers of 73 and 92 W. In this case, the exposure time t_r of the reaction mixture was varied at a fixed radiation power. The absorbed energy Q was calculated from the relationship

$$Q = Wt_r - Q_1 - Q_2,$$

where W is the radiation power at the cell inlet; Q_1 and Q_2 are the energies detected by calorimeter *7* in the course of sequential reflection and transmission measurements (Fig. 1). At an ethane conversion of ≥8%, the fraction of absorbed energy was 80–97%, and it depended on the initial mixture composition, radiation power, and exposure time. Figure 2 also has an additional axis on which absorbed energy per mole of starting reactants is plotted. The number of moles was

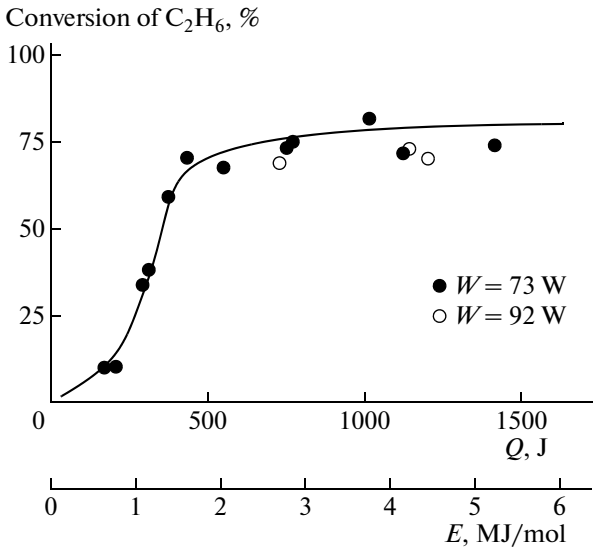

Fig. 2. Dependence of the degree of ethane conversion on the absorbed energy Q or the energy E per mole of the reaction mixture. The composition of the starting mixture, vol %: C_2H_6, 91; C_2H_4, 9.

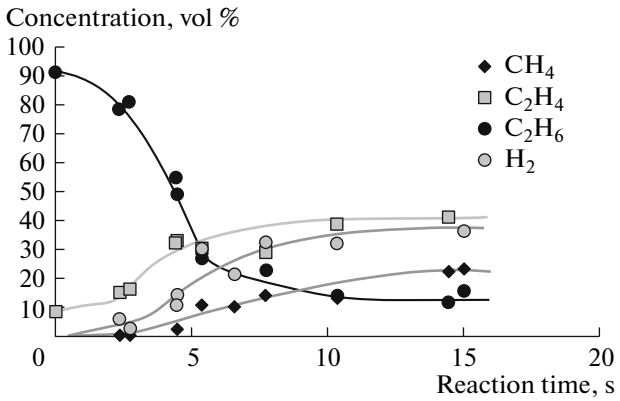

Fig. 3. Experimental data on changes in the composition of an ethane–ethylene mixture under the action of a laser beam with a power of 73 W. The composition of the starting mixture, vol %: C_2H_6, 91; C_2H_4, 9.

calculated based on the quartz cell volume of 6 cm^3 under normal conditions.

At an ethane conversion of about 10%, approximately 150 J of laser radiation energy was absorbed in the reactor (Fig. 2). A further increase in absorption to 500 J was accompanied by a dramatic increase in the conversion of ethane to 60–65%. If the input energy was higher than 500 J and increased up to 1500 J, a maximum conversion of 75% was reached, which depended only slightly on the absolute value of Q over the specified interval.

Figure 3 shows the dependence of the composition of the ethane–ethylene mixture on exposure time at a laser output power of 73 W and an initial C_2H_4 concentration of 9 vol %. At exposure times to 5 s, the fraction of methane in the reaction mixture slowly increased with respect to the fractions of hydrogen and ethylene, and it was as high as a few percent. As a 30% ethylene volume fraction was reached, the methane content increased to 10% by the sixth second and then slowly increased to 22%. Hydrogen appeared 2.5 s after the onset of irradiation, and its concentration gradually increased to 35%. The concentration of ethylene was as high as 40% at a residual ethane fraction of 12%.

The results were almost independent of the initial concentration of ethylene over the range of 6–15 vol %. At the concentrations of ethylene lower than 6 vol %, ethane was not dehydrogenated in the irradiated mixture and hydrogen did not appear. The dependence of the conversion of ethane on absorbed dose remained unchanged as the power of laser radiation was increased. In this case, the exposure time required for reaching a maximum ethylene content of the final mixture became shorter. Methane and hydrogen also appeared at shorter exposure times.

DISCUSSION

Thermal Physics of the Reactor

Laser energy relaxation. Let us evaluate the possible role of multiphoton processes under conditions of our experiments in terms of the parameter $\zeta = N_\lambda / N_{n_1}$, where N_λ is the number of laser radiation photons absorbed in the volume $\sim Ld^2$ during the time τ between two molecular collisions; $N_{n_1} = n_1 Ld^2$ is the number of ethylene molecules in this volume; n_1 is the concentration of ethylene; and $d \approx 11$ mm is the laser beam diameter in the cell. On condition that the Bouguer–Lambert–Beer law is applicable, that is, at a small number of excited molecules in the volume during the observation time, the energy transferred to the gas at length L at a low absorption level is $E \approx \alpha n_1 WL\tau$. The number of photons $N_\lambda \approx \alpha n_1 WL\tau / E_0$, where $E_0 \approx 2 \times 10^{-20}$ J is the photon energy of CO_2-laser radiation, and W is the laser power. In the case of an ideal gas, $\tau^{-1} \approx \sigma(n_1 + n_2) v_t$, where $\sigma \approx 2 \times 10^{-15}$ cm^2 is the gas-kinetic cross section [14]; v_t is the thermal velocity of molecules; and n_2 is the concentration of a buffer gas. In calculations for accurate evaluation, we assume that $n_1 + n_2 = n \approx$ const. Then, the following relation for the parameter ζ is true:

$$\zeta = N_\lambda / N_{n_1} = \alpha W / E_0 d^2 \sigma n v_t.$$

At the radiation power density $W/d^2 \approx 50$ W/cm^2, the atmospheric pressure of gases, the above value of α, and the ethylene concentration of ~10%, we obtain $\zeta \approx 10^{-7}$.

Thus, even at a very low probability of vibrational–translational relaxation (Molin et al. [15] estimated this probability for methane at $\sim 5 \times 10^{-5}$ and the relax-

ation time of the $C_2H_4^*$ excited molecule in a gas at 10^{-5}–10^{-4} s), the fraction of excited molecules is low and multiphoton processes cannot occur under conditions of our experiments. Consequently, energy transfer to a gas by the absorption of laser radiation under our conditions is a solely thermal process. Qualitatively, these conclusions remain unchanged as the temperature is increased by a factor of 3–4.

Thermal balance. A reactor with laser energy input is characterized by the axial distribution of the heat source and the gas isolation of walls from the reaction zone. Let us evaluate the heat flow through an isolating gas layer to reactor walls in the absence of chemical transformations from this layer. It is well known that the considerable temperature dependence of the heat capacity c_p and the thermal conductivity coefficients k_t of ethylene, methane, and other molecular gases over the temperature range of 300–1200 K [16]. Thus, for ethane at $T_0 = 300$ K,

$$c_p \approx 53\ (1 + 1.9 \times 10^{-3}(T - T_0))\ \text{J mol}^{-1}\ \text{K}^{-1},$$

$$k_t \approx 21 \times 10^{-3}(T/T_0)^{1.73}\ \text{W mol}^{-1}\ \text{K}^{-1}.$$

In this case, the thermal diffusivity $\chi = k/c_p\rho$ changed by a factor of about 3 for ethane in a temperature range from 300 to 1000 K (ρ is the gas density). The settling time of a thermal field (τ_1) at characteristic distance h can be estimated from the relationship $h \approx 2(\chi\tau_1)^{1/2}$. Hence, at an axial reactor geometry and $h = (D - d)/2$, we find $\tau_1 = \rho(D - d)^2c_p/16k_t$. At 800 K, we obtain $\tau_1 \approx 0.2$ s. If the radiation power absorbed in a gas is 50 W, heating to a temperature higher than 1300 K will occur for the time τ_1 (on condition that the absorption coefficient is constant in the absence of heat transfer to the reactor walls and the absence of chemical reactions with consideration for the thermal dependence of c_p). The temperature of reactor walls measured in the course of experiments was no higher than 400 K. At these temperatures, the thermal energy flow to the reactor walls through an isolating gas layer with an axial geometry is

$$W_1 \approx 2\pi Lk_t\ (T - T_0)/(1 - d/D)$$

$$\approx 0.12L(T - T_0)(T/T_0)^{1.73}/(1 - d/D) \approx 40\ \text{W}.$$

Except for heat losses, which should be taken into account at any exposure times, this calculation allows us to estimate the lowest power absorbed in the volume required for the onset of pyrolysis.

As found by experiments, at $W \leq 35$ W, the conversion of ethane was not observed even at a long exposure (longer than 5 min) to laser radiation. At the incident radiation power $W \approx 73$ W, a detectable ethane conversion was reached only at an exposure time longer than 2 s. The experimental data shown in Fig. 2 suggest that the threshold energy that should be supplied to the reaction mixture in order to initiate a reaction is $Q \approx 500$–585 kJ/mol. If more than a half of this energy is lost on the walls because of thermal conductivity, ~250 kJ/mol remained for chemical reactions. This energy is supplied to the reactor with a power flow to 100 W/cm^2. In standard tube reactors for pyrolysis, the power flow used for supplying thermal energy to the reaction mixture through the reactor wall is usually lower by one and a half or two orders of magnitude.

Temperature conditions. Let us estimate the temperature at the reactor center assuming a heat flow to the walls because of thermal conductivity and the absence of chemical reactors. The numerical solution of the problem of a radial temperature distribution at bulk heat release with a power of 80 W indicates that the gas temperature at the reactor axis is 900–1050 K. At these temperatures, ethane dehydrogenation should occur at a noticeable degree. The calculated temperature at the reactor axis depends only slightly on the wall temperature, which was varied over a range from 300 to 600 K in the calculations. An increase in the heat release power from 60 to 100 W expands the high-temperature zone along the reactor radius rather than increases a maximum temperature. At high hydrogen concentrations in the mixture, the thermal conductivity increases and the maximum temperature decreases by more than 100 K.

Because the gas temperature changes in a direction from the reactor axis to the walls, a difference between the rates of chemical reactions at various points appears in the reactor volume. This difference can be smoothed because of the diffusion exchange of reactants with characteristic times longer than the characteristic settling time of heat flows (0.2 s). Using the empirical dependence of the degree of thermal conversion of ethane on reaction time

$$\text{d}(\ln[C_2H_6])/\text{d}t = 10^{14.5}\exp(-34.16/10^{-3}T)\ [\text{s}^{-1}],$$

which was given in a monograph by Zhorov [1], and evaluating the time τ_2 during which the concentration of ethane decreased by a factor of e ($\tau_2 \approx 3$ s) under conditions of our experiments, we found that the characteristic temperature at the reactor center was $T \approx 990$ K.

Gas-Phase Reaction Kinetics

The dehydrogenation of ethane in a gas phase is traditionally described by a radical chain mechanism [1–9] assuming that the process is initiated as a result of the thermal dissociation of starting reactants with the formation of free radicals; thereafter, chain propagation and termination reactions also occur with the participation of free radicals. For industrial processes that occur at atmospheric pressure and in which high ethane conversions are reached, a reaction scheme was recommended. Table 1 summarizes this scheme and the rate constants of corresponding steps [1].

With the use of this scheme, we calculated changes in the concentrations of ethane pyrolysis products depending on reaction time by the ChemPak program package [17], which allowed us to generate a set of differential rate equations and to choose a numerical

Table 1. Conventional reaction scheme of a radical chain mechanism of ethane pyrolysis and the rate constants of corresponding reactions [1]

Step no.	Reaction	$\log k$ ($19.14 \times 10^{-3}T^{-1}$)	Dimensionality of k
	Chain initiation		
1	$C_2H_6 \longrightarrow 2\dot{C}H_3$	$\log k_1 = 16.0 - 360$	s^{-1}
	Chain propagation		
2	$\dot{C}H_3 + C_2H_6 \longrightarrow \dot{C}_2H_5 + CH_4$	$\log k_2 = 10 - 50$	$l\,mol^{-1}\,s^{-1}$
3	$\dot{C}_2H_5 \longrightarrow C_2H_4 + H^{\cdot}$	$\log k_3 = 13.5 - 170$	s^{-1}
–3	$H^{\cdot} + C_2H_4 \longrightarrow \dot{C}_2H_5$	$\log k_{-3} = 10.4 - 8.4$	$l\,mol^{-1}\,s^{-1}$
4	$H^{\cdot} + C_2H_6 \longrightarrow H_2 + \dot{C}_2H_5$	$\log k_4 = 11 - 40$	$l\,mol^{-1}\,s^{-1}$
5	$\dot{C}H_3 + C_2H_4 \longrightarrow \dot{C}_3H_7$	$\log k_5 = 8.5 - 33$	$l\,mol^{-1}\,s^{-1}$
–5	$\dot{C}_3H_7 \longrightarrow \dot{C}H_3 + C_2H_4$	$\log k_{-5} = 13.9 - 137$	s^{-1}
	Chain termination		
6	$2\dot{C}_2H_5 \longrightarrow C_2H_4 + C_2H_6$	$\log k_6 = 11.5 - 8.4$	$l\,mol^{-1}\,s^{-1}$

Note: Somewhat different, but similar, values of the rate constants of gas-phase reactions are given in the NIST database [18].

method for integrating them. Figure 4 shows the results. For a total pressure of 1 bar and a temperature of 1033 K, a quasi-steady state in an isobaric process was established after about 20 s. This time strongly depends on temperature. Thus, at 1093 K, the characteristic time shortened to 3 s. The chain length in terms of the methyl radical (the ratio of the overall rate of ethylene synthesis to the rate of thermal radical initiation) at 1033 K was $\nu \approx 10$.

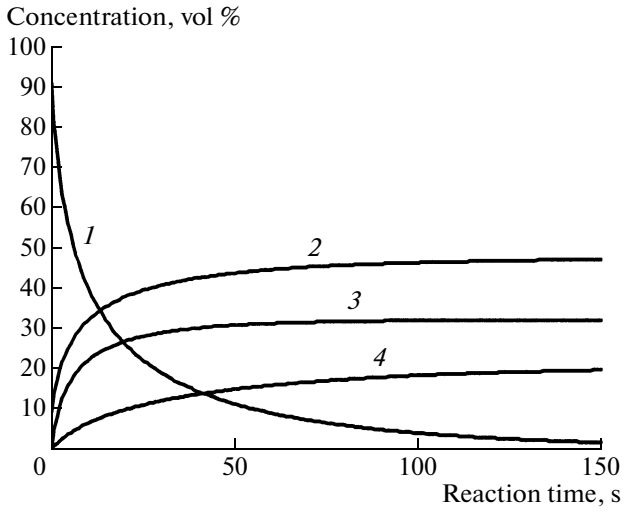

Fig. 4. Calculated data on changes in the reaction mixture composition in the course of ethane pyrolysis occurring by a radical chain mechanism [1] (see Table 1): (*1*) C_2H_6, (*2*) C_2H_4, (*3*) H_2, and (*4*) CH_4. The calculation was performed as applied to an isobaric process at 1 bar and 1033 K.

The above calculated product concentrations are quantitatively and qualitatively inconsistent with empirical data obtained in the pyrolysis of ethane performed in industrial furnaces [9]. Thus, the calculated conversion of ethane at 1033 K and a pyrolysis time of 1 s was 9%, whereas it was as high as 32% in an industrial reactor under the same conditions [9]. According to empirical data, the reaction products were formed at moderate ethane conversions in the following ratio:

$$0.9C_2H_4 + 0.9H_2 + 0.11CH_4 + 0.0167C_3H_6 + 0.01C_4H_6.$$

As can be seen, the concentrations of ethylene and hydrogen were approximately the same, whereas the concentration of methane was lower than that of ethylene by a factor of 9. Such a distribution of reaction products was also found in our experiments performed in the absence of heterogeneous reactions at the walls. In our experiments, only C_4 hydrocarbons and heavier compounds were not formed.

The reaction scheme of ethane pyrolysis in which the reaction of chain termination (Table 1, step 6) is replaced by the step

$$H^{\cdot} + \dot{C}_2H_5 \longrightarrow C_2H_6,$$

with the rate constant [1] $k = 10^{14}\exp(-14.91/10^{-3}T)$ $l\,mol^{-1}\,s^{-1}$ has been often considered in the literature (e.g., see [2]). Our calculations demonstrate that, in accordance with this scheme, ethylene and hydrogen will be formed in the same concentrations, whereas the methane content of the mixture will be no

Table 2. Thermodynamic parameters of chemical reactions occurring in the pyrolysis of ethane

Step no.	Reaction	$\Delta_r H^0_{298}$, kJ/mol	$\Delta_r S^0_{298}$, J mol^{-1} K^{-1}	$\Delta_r G^0_{1000}$, kJ/mol
1	$C_2H_6 \longrightarrow 2\dot{C}H_3$	381.6	160.02	221.8
1a	$C_2H_4 + C_2H_6 \longrightarrow \dot{C}H_3 + \dot{C}_3H_7$	283.7	36.4	247.4
2	$\dot{C}H_3 + C_2H_6 \longrightarrow \dot{C}_2H_5 + CH_4$	−16.7	11.6	−28.2
3	$\dot{C}_2H_5 \longrightarrow C_2H_4 + H^{\cdot}$	148.4	85.6	62.8
4	$H^{\cdot} + C_2H_6 \longrightarrow H_2 + \dot{C}_2H_5$	−11.6	35.7	−47.3
5	$\dot{C}H_3 + C_2H_4 \longrightarrow \dot{C}_3H_7$	−97.9	−123.6	25.7
6	$2\dot{C}_2H_5 \longrightarrow C_2H_4 + C_2H_6$	−277.6	−49.1	−228.6
7	$\dot{C}_2H_5 + C_2H_6 \longrightarrow \dot{C}_2H_5 + C_2H_4 + H_2$	136.8	121.2	15.6

Note: The standard changes in enthalpy $\Delta_r H^0_{298}$, entropy $\Delta_r S^0_{298}$, and Gibbs energy $\Delta_r G^0_{1000}$ were calculated from reference data on the thermodynamic properties of elementary substances [14].

higher than 0.1 vol %. This ratio between the products is due to a sufficiently great chain length (ν = 500–1000); however, it is inconsistent with experimental data obtained at considerable degrees of ethane conversion. Thus, the applicability of the above kinetic schemes to the conditions of both our experiments and industrial processes at a high yield of pyrolysis products and $T \le 1050$ K should be additionally substantiated and the schemes should be modified. In such a situation, kinetic schemes are usually supplemented with molecular steps to perform practical calculations [9].

The supply of thermal energy to the reactor designed for performing endothermic reactions through the reactor walls results in the participation of surfaces heated to high temperatures in the process. This creates possibilities for the effect of heat- and mass-transfer processes on the kinetics of heterogeneous and gas-phase reactions in tube furnaces. However, in our experiments, where heterogeneous reactions at the walls had no effect on the process, the ratio between the main pyrolysis products (hydrogen, methane, and ethylene) was qualitatively the same as the ratio between these products in tube reactors. This fact suggests that the observed product yields depend on the gas-phase reactions rather than heat- and mass-transfer processes.

Table 2 summarizes the thermodynamic parameters of the most important reactions of the test process, including the calculated values of Gibbs energy changes at 1000 K. These calculations were semiquantitative because they did not take into account the temperature dependence of thermal conductivity. It is believed that the pyrolysis of ethane primarily depends on radical generation reactions. Thus, the formation of $\dot{C}H_3$ radicals from the ethane molecule in accordance with the first reaction is the most energy-consuming step ($\Delta_r H^0_{298}$ = 381.6 kJ/mol). However, an even greater energy is required for the abstraction of a hydrogen atom from ethane. At considerable degrees of ethane conversion, bimolecular reactions with the participation of pyrolysis products, for example, ethylene, can be among the reactions that initiate a chain radical process. Indeed, Semenov [8] noted that the presence of ethylene considerably increased the concentration of ethyl radicals, which were formed in the reaction (the reverse of reaction 6 in Table 2)

$$C_2H_4 + C_2H_6 \longrightarrow 2\dot{C}_2H_5.$$

Because the activation energy of this reaction in the direction from right to left is close to zero, the activation energy in the direction from left to right can be equated to the enthalpy of an endothermic reaction, namely, 277.6 kJ/mol, which is much lower than the activation energy of step 1. Therefore, the appearance of ethane in the reaction mixture increases the concentration of ethyl radicals. According to published data [1], the rate constant of reaction 6 in the direction from right to left is described by the expression $\log k_{-6} = 11.5 - 8.4/(19.14 \times 10^{-3}T)$ [l mol^{-1} s^{-1}]. Nevertheless, if reaction (6) in the opposite direction is taken into consideration in the reaction scheme of pyrolysis, the results of calculations remain almost unchanged because step –6 mainly affects only the concentration of ethyl radicals.

At the same time, another reaction between C_2H_4 and C_2H_6 can occur to yield propyl and methyl radicals (Table 2, step 1a). The change in the Gibbs energy of this reaction at 1000 K is only slightly greater than

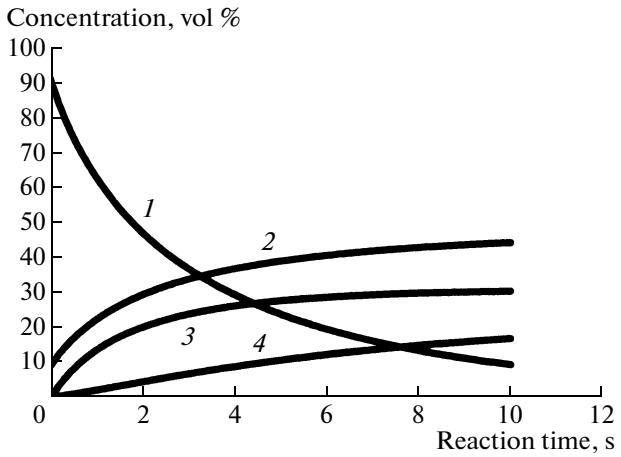

Fig. 5. Calculated data on changes in the reaction mixture composition in the course of gas-phase ethane pyrolysis occurring by an autocatalytic radical mechanism at 990 K: (*1*) C_2H_6, (*2*) C_2H_4, (*3*) H_2, and (*4*) CH_4.

$\Delta_r G^0_{1000}$ in reaction 1 and in the reverse of step 6. The enthalpy change in reaction 1a is approximately 100 kJ/mol smaller than that in the reaction of ethane degradation into two methyl radicals. Thus, this channel of the formation of methyl radicals can became more preferable than reaction 1 as the ethylene concentration is increased.

We propose the following reaction scheme for the autocatalytic radical mechanism of ethane pyrolysis:

Chain initiation

$$1.\ C_2H_6 \longrightarrow 2\dot{C}H_3$$

$$1a.\ C_2H_4 + C_2H_6 \longrightarrow \dot{C}_3H_7 + \dot{C}H_3$$

Chain propagation

$$2.\ \dot{C}H_3 + C_2H_6 \longrightarrow \dot{C}_2H_5 + CH_4$$

$$3.\ \dot{C}_2H_5 \longrightarrow C_2H_4 + H^{\cdot}$$

$$-3.\ H^{\cdot} + C_2H_4 \longrightarrow C_2H_5$$

$$4.\ H^{\cdot} + C_2H_6 \longrightarrow H_2 + \dot{C}_2H_5$$

$$5.\ \dot{C}H_3 + C_2H_4 \longrightarrow \dot{C}_3H_7$$

$$-5.\ \dot{C}_3H_7 \longrightarrow \dot{C}H_3 + C_2H_4$$

Chain termination

$$6.\ 2\dot{C}_2H_5 \longrightarrow C_2H_4 + C_2H_6$$

The composition of the reaction mixture at 990 K was calculated in accordance with this scheme with the use of the rate constant of reaction 1a chosen in the form $\log k_{1a} = 13.4 - 247.4/(19.14 \times 10^{-3}\ T)$ [l mol^{-1} s^{-1}]. Figure 5 shows the results (Table 1 summarizes the rate constants of the other steps). As can be seen in Fig. 5, the special features of the reaction that follow from the calculation (a quasi-steady-state regime, the consumption of starting reactants, and the buildup of products in the course of the reaction) are generally consistent with the experimental data. The rate of formation of $\dot{C}H_3$ radicals by reaction 1a becomes higher than the rate of reaction 1 at the ethylene concentration $[C_2H_4] > k_1/k_{1a} \approx 5.2 \times 10^{-4}$ mol/l. At 1000 K and 1 bar, this value corresponds to $[C_2H_4] \approx 4$–5 vol %, that is, the experimentally observed threshold concentration of ethylene. This threshold concentration suggests that reaction 1a is of importance for the initiation of a radical chain reaction at high ethane conversions and under the conditions of our experiments. The difference between calculated (Fig. 5) and experimental (Fig. 3) dependences at the initial stage of the reaction was due to the fact that the calculation was performed based on the assumption of an isothermal process. However, in real experiments, a considerable fraction of radiation power was consumed for the heating of the reactor and the gas mixture at the initial point in time after a laser was turned on.

Thus, at a sufficiently high concentration of ethylene, methyl radicals can form via a competitive reaction path, which is characterized by milder parameters. An increase in the concentration of methyl radicals in the reaction zone results in an increase in the concentration of ethyl radicals, which are a key species in chain propagation reactions (Table 2, steps 3 and 4). The propyl radical serves as a source for the formation of propylene and acetylene, which also occur among the products of ethane pyrolysis. In addition, the enthalpies of the reverse of reaction –6 (278 kJ/mol) and reaction 1a (284 kJ/mol) are close to the experimentally found energy of ~250 kJ/mol, which was consumed in our experiments for performing chemical transformations in the mixture.

The appearance of ethylene in the reaction mixture produces additional reaction paths for the generation of radicals in bimolecular reactions. According to the reaction scheme proposed, ethylene and hydrogen are formed in equal amounts, whereas the methane content is three times lower. This distribution of reaction products is consistent with both the results of our experiments and the composition of reaction mixture components in industrial plants. The calculated character of changes in the course of ethane conversion and the buildup of reaction products at a temperature of 990 K are close to our experimental data. Note that, in accordance with the reaction scheme given in Table 1, the time taken to reach approximately the same changes in the reaction mixture composition at 990 K is longer than that at 1033 K by a factor of tens.

The set of reactions in the proposed scheme can be considered as an autocatalytic process with respect to ethylene. The kinetic characteristics of an autocatalytic process are usually consistent with the characteristics of radical chain reactions. The chain length corresponding to the proposed mechanism of ethane pyrolysis is 20–30 units, which actually suggests a radical chain reaction mechanism with short chains. The above value of the rate constant of chemical reaction 1a is semiquantitative because the concentrations of components in experiments where the temperature profile of a reaction zone is considered are averaged values.

The results of the above experiments suggest that the conventional radical chain mechanism of ethane dehydrogenation [1, 2, 9] is true only if the following conditions are met: (1) a reduced partial pressure of ethane; (2) the presence of inert diluents, in particular, argon; (3) a high temperature; (4) a low degree of conversion at which the effect of products on the reaction kinetics is insignificant; and (5) the participation of heterogeneous reactions at the walls of the reaction vessel, which are responsible for energy supply for performing endothermic reactions. The gas-phase thermal dehydrogenation of ethane in the absence of diluents at atmospheric pressure is described by an autocatalytic mechanism with respect to ethylene. We experimentally found that the conversion of C_2H_6 was as high as 75% in the thermochemical gas-phase reaction of ethane dehydrogenation at atmospheric pressure in a wall-less reactor to which laser radiation with an energy density to 100 W/cm^2 was supplied.

ACKNOWLEDGMENTS

We are grateful to G.M. Zhidomirov, V.I. Avdeev, and A.G. Okunev for helpful discussions and remarks. This work was performed in the framework of integration project no. 44 of the Siberian Branch of the Russian Academy of Sciences (coordinator: V.M. Fomin); it was supported in part by the Ministry of Education and Science (RNP.2.1.1.1969) and the Presidium of the Russian Academy of Sciences (program no. 18-2).

REFERENCES

1. Zhorov, Yu.M., *Kinetika promyshlennykh organicheskikh reaktsii: Spravochnoe izdanie* (Kinetics of Industrial Organic Reactions: A Handbook), Moscow: Khimiya, 1989.
2. Laidler, K., *Chemical Kinetics*, New York McGraw-Hill, 1950.
3. Shevel'kova, L.V., Gusel'nikov, L.E., Bakh, G., and Tsimmermann, G., *Usp. Khim.*, 1992, vol. 61, no. 4, p. 792.
4. Zaslonko, I.S., Smirnov, V.N, and Tereza, A.M., *Kinet. Katal.*, 1994, vol. 35, no. 1, p. 5.
5. Parkhomenko, V.D., Soroka, P.I., Krasnokutskii, Yu.I., et al., *Plazmokhimicheskaya tekhnologiya* (Plasma Chemical Technology), Novosibirsk: Nauka, 1991.
6. Barltrop, J. and Coyle, J., *Excited States in Organic Chemistry*, London: Wiley, 1975.
7. Reutov, O.A., Kuri, A.L., and Butin, K.P., *Organicheskaya khimiya* (Organic Chemistry), Moscow: Binom, 2004.
8. Semenov, N.N., *Tsepnye reaktsii* (Chain Reactions), Moscow: Nauka, 1986.
9. Mukhina, T.N., Barabanov, N.L, Babash, S.E., et al., *Piroliz uglevodorodnogo syr'ya* (Pyrolysis of Hydrocarbon Stocks), Moscow: Khimiya, 1987.
10. Mantashyan, A.A., Khachatryan, L.A., and Sukasyan, A.A., *Kinet. Katal.*, 1989, vol. 30, no. 2, p. 272.
11. Bobrov, N.N., Leonov, A.S., Belov, A.N., et al., *Katal. Prom–sti.*, 2005, no. 2, p. 50.
12. Gunaze, O.A. and Trofimov, V.A., *Zh. Tekh. Fiz.*, 1999, vol. 69, no. 4, p. 65.
13. *NIST Chemistry Web Book*, http://webbook.nist.gov.
14. Ravdel', A.A. and Ponamareva, A.M., *Kratkii spravochnik fiziko-khimicheskikh velichin* (Concise Handbook of Physicochemical Quantities), St. Petersburg: Ivan Fedorov, 2002.
15. Molin, Yu.N., Panfilov, V.N., and Petrov, A.K., *Infrakrasnaya fotokhimiya* (Infrared Photochemistry), Novosibirsk: Nauka, 1985.
16. Grigor'ev, I.S. and Meilikhov, U.Z., *Fizicheskie velichiny* (Physical Quantities), Moscow: Energoatomizdat, 1991.
17. Vshivkov, V.A., Sklyar, O.P., Snytnikov, V.N., and Chernykh, I.G., *Vych. Tekhnol.*, 2006, vol. 11, no. 1, p. 35.
18. http://kinetics.nist.gov/kinetics/.